Caleta Olivia- Wave Runup Report

January 2, 2025

This report is compiled with the results of the CoastSat.Venice tool for the calculation of runup values for paleo sea-level applications (Rovere, 2024), available at this link. The tool is based upon the work of Vos et al. (2019, 2020) for the slope extraction from satellite data, on the runup models implemented in Leaman et al. (2020) and on the tidal and wave models shown below. For a case study, see

Water levels

Water level data were extracted at the coordinates and over the period shown in Table 1 using the FES2022 global tidal model (Carrere et al., 2022) at a point slightly offshore of Caleta Olivia.

Property	Value
Latitude	−46.537156
Longitude	−67.441463
Start date-time	1980-01-01T00:00:00+00:00
Start date-time	2024-10-31T00:00:00+00:00

Table 1: Location of water level extraction point and dates of water level extraction for Caleta Olivia.

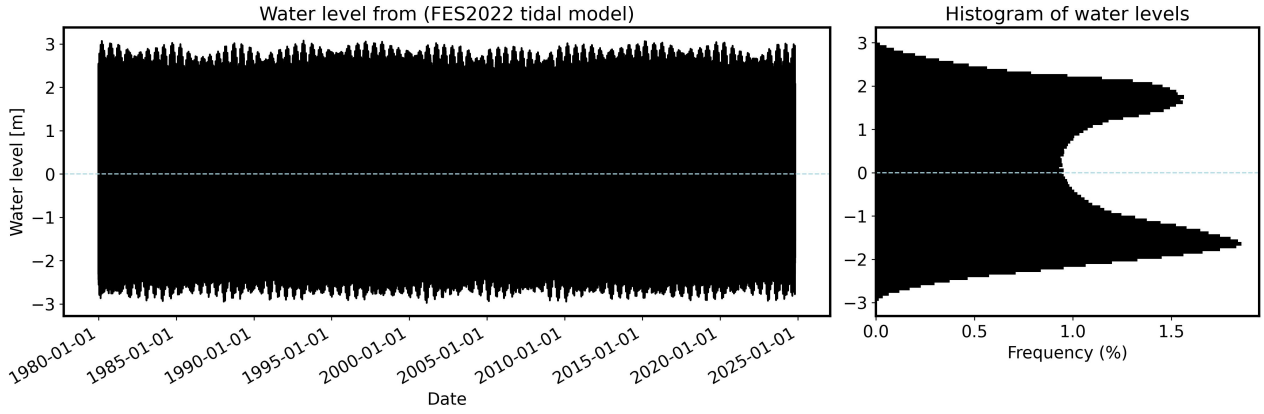

Figure 1: Water levels extracxted from the FES22 tidal model for Caleta Olivia. Left: water level time series. Right: Histogram of water level data. Blue dashed line represents mean tidal level (MTL).

Wave data

Wave data is retrieved from the Copernicus Marine Environment Monitoring Service (CMEMS) WAVeReanalYSis (WAVERYS, Law-Chune et al., 2021). WAVERYS takes into account oceanic currents from the GLORYS12 physical ocean reanalysis (Lellouche et al., 2018) and assimilates wave heights from altimetry missions and directional wave spectra from Sentinel 1 synthetic aperture radar from 2017 onwards. This dataset spans the last ~43 years (01 Jan 1980 to 30 Sept 2023). The wave data was sampled at a virtual buoy slightly offshore Caleta OliviaTable 2, and the average wave height, period and direction is shown in Figure 2.

Property	Value
Latitude	−45.987233
Longitude	−64.434815

Table 2: Coordinates of water level extraction point for Caleta Olivia.

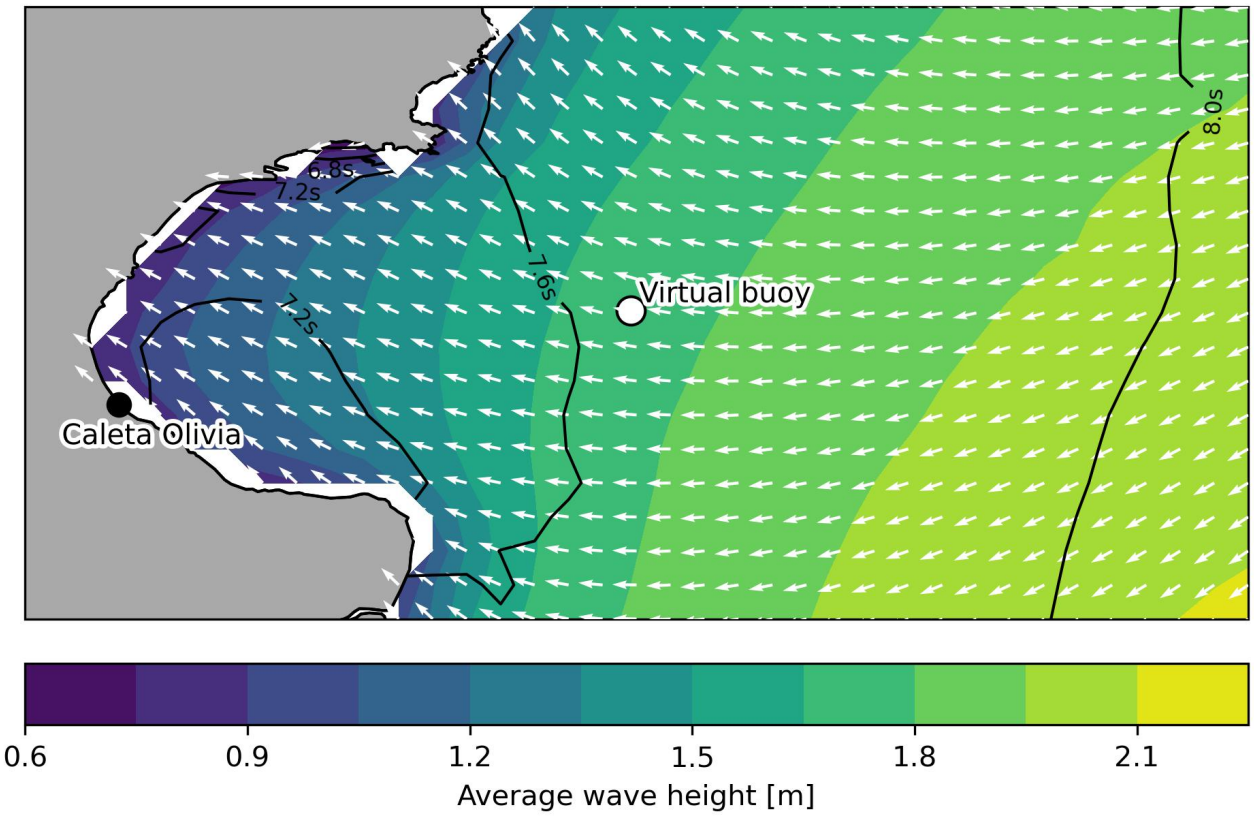

Figure 2: Average wave height (colored countours), period (black line with labels) and direction (arrows) extracted for the area of interest from the WAVERYS data. In the figure are shown the location of the virtual buoy (coordinates in Table 2) and the location of the site of interest.

The wave data at the virtual buoy was culled to include only the waves directed perpendicularly to the shore (Figure 3, right panels). Those are the data used to calculate the runup on the coast. The wave rose is shown in Figure 4.

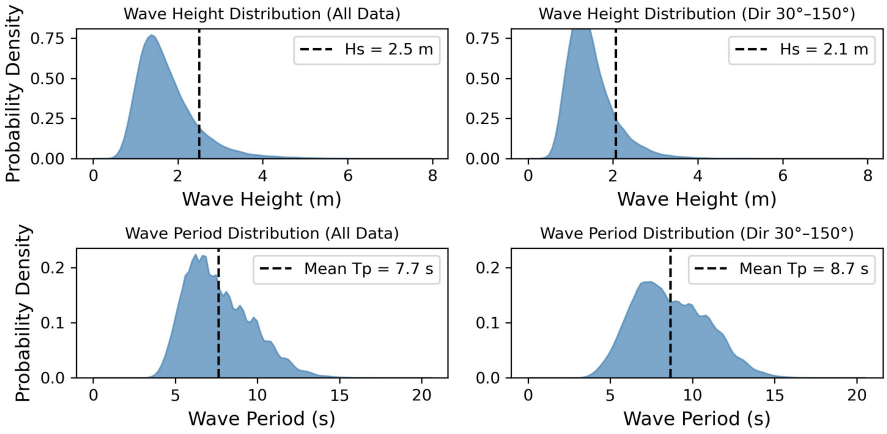

Figure 3: Left panels: probability distribution of wave height (upper) and period (lower) for all the wave directions in the study area. Right panels: the same are left panels, but only for the directions more perpendicular to the coast.

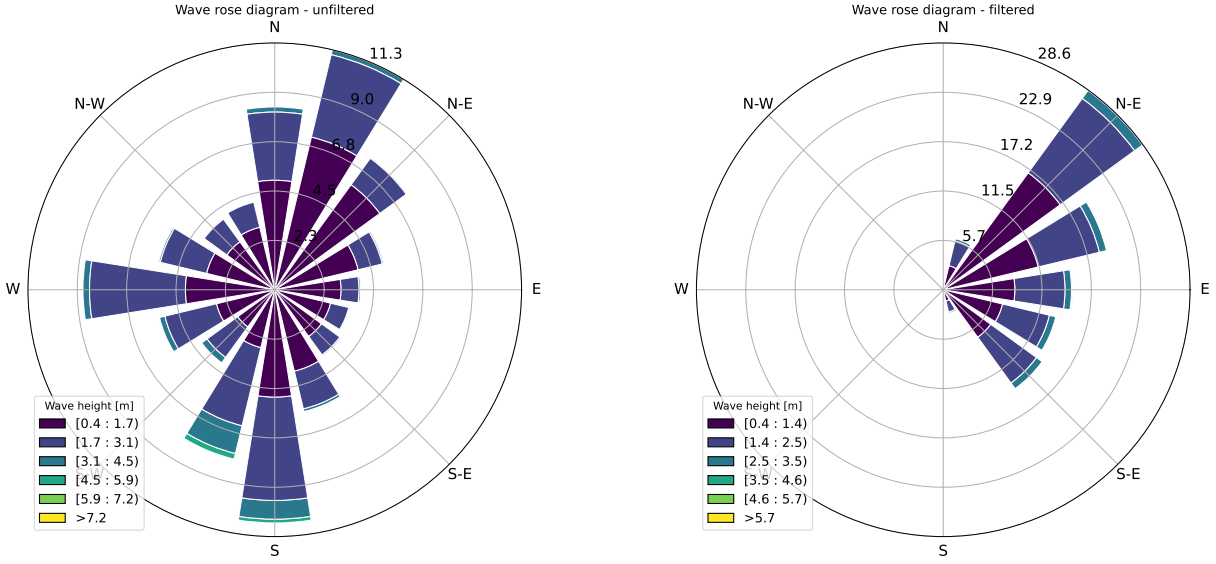

Figure 4: Left: wave rose, unfiltered for wave direction, at the virtual buoy. Right: same, filtered for shore-perpendicular wave directions.

Beach slope

The beach slope was calculated from transects derived from CoastSat.Slope , shown in Table 3. The slope was sampled within the confidence intervals with a random triangular sampling as shown in Figure 5.

Transect #	CI Lower (5%)	CI Upper (95%)	Slope Average
1	0.0785	0.0885	0.081
2	0.076	0.0835	0.081
3	0.0735	0.081	0.076
4	0.071	0.076	0.076
5	0.076	0.0835	0.081

Table 3: Beach slope and confidence intervals for each beach transect at the site of interest.

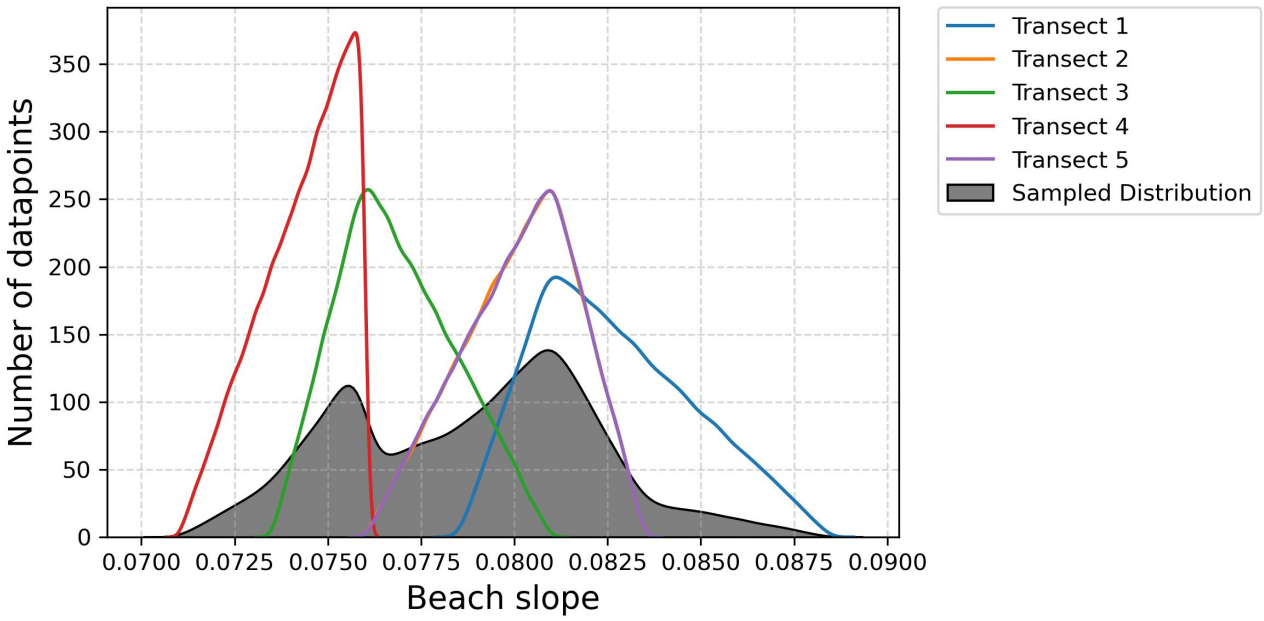

Figure 5: Slope distribution used in runup calculations (gray area) and slope of each single transect (colored lines).

Runup calculations

The runup is calculated for the modern wave conditions with nine different models (Stockdon et al., 2006; Vousdoukas et al., 2012; Holman, 1986; Power et al., 2019; Passarella et al., 2018; Senechal et al., 2011; Atkinson et al., 2017; Ruggiero et al., 2001; Nielsen, 2009). These are shown separately in Figure 6.

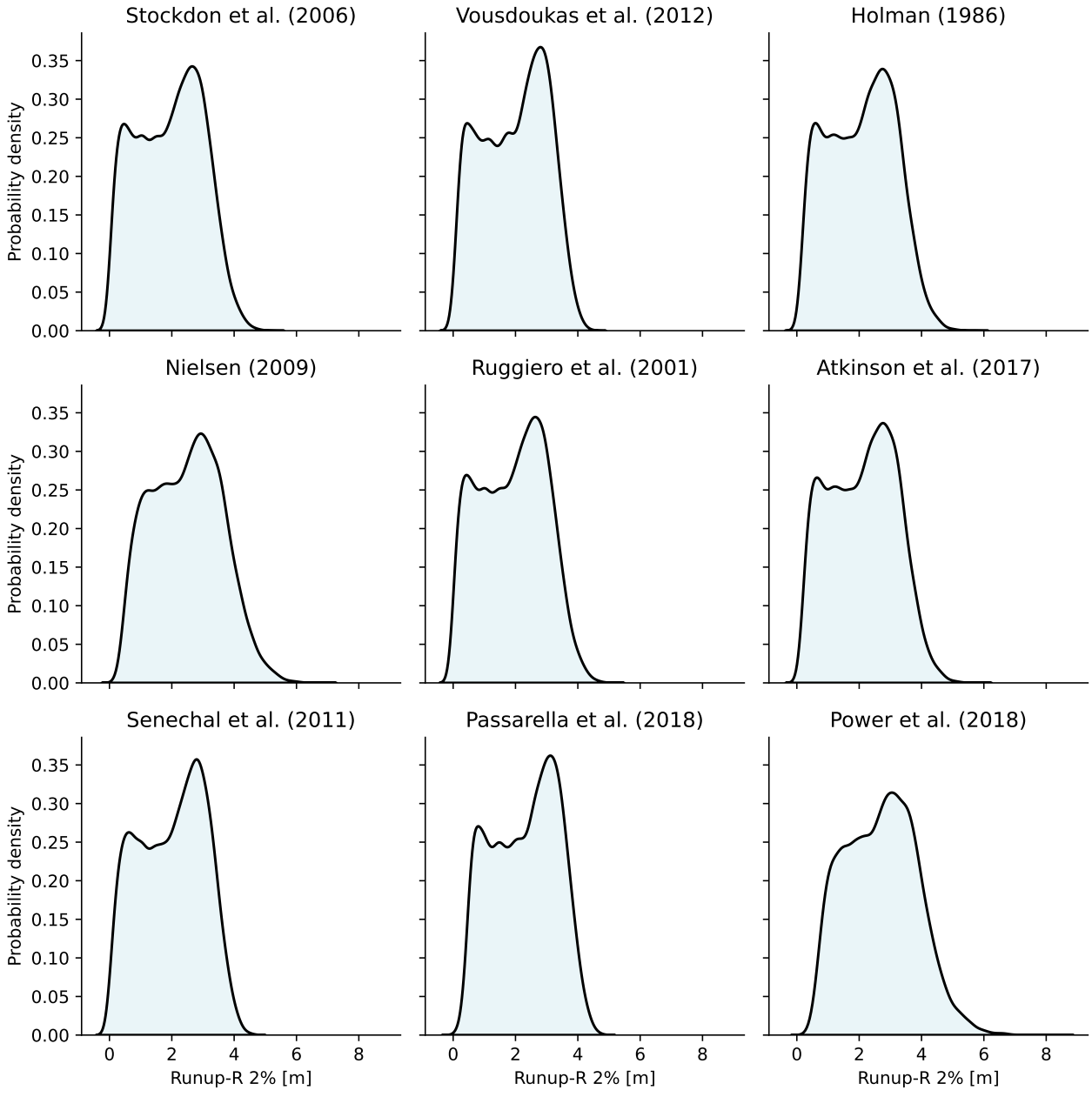

Figure 6: Modern runup calculated using nine empyrical models combined with wave and tide data atthe site of interest.

The runup over longer time period (synthetic runup) is shown in Figure 7, alongside with the cumulative modern runup derived merging the probability distributions shown in Figure 6.

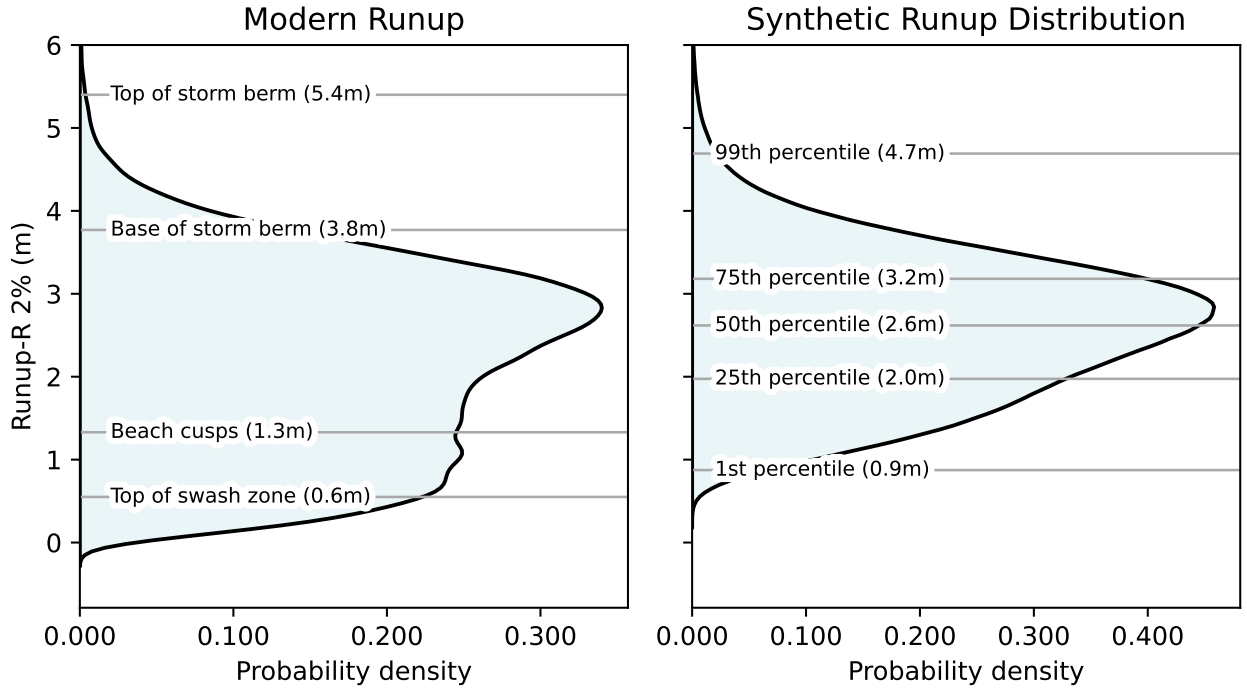

Figure 7: A) Probability density plots representing simulated 2% wave runup (R2) at Caleta Oliviabetween 1980 and 2024, for waves with directions between NNE and SSE and reaching the coast in tidal conditions from MSL to high tide. Elements measured on the modern shoreline (if present) are plotted as grey lines with labels. Right) Probability density plot representing simulated 2% wave runup at Caleta Oliviafor the synthetic dataset, calculated as described in the main text. The grey lines show the 1st, 25th, 50th, 75th and 99th percentiles of this distribution.

References

Atkinson, A. L., H. E. Power, T. Moura, T. Hammond, D. P. Callaghan, and T. E. Baldock (2017). Assessment of runup predictions by empirical models on non-truncated beaches on the south-east Australian coast. *Coastal Engineering 119*, 15–31.

Carrere, L., F. Lyard, M. Cancet, D. Allain, M.-L. Dabat, E. Fouchet, E. Sahuc, Y. Faugere, G. Dibarboure, and N. Picot (2022). A new barotropic tide model for global ocean: Fes2022. In *2022 Ocean Surface Topography Science Team Meeting*, pp. 43.

Holman, R. (1986). Extreme value statistics for wave run-up on a natural beach. *Coastal Engineering 9*(6), 527–544.

Law-Chune, S., L. Aouf, A. Dalphinet, B. Levier, Y. Drillet, and M. Drevillon (2021). WAVERYS: a CMEMS global wave reanalysis during the altimetry period. *Ocean Dynamics 71*, 357–378.

Leaman, C., T. Beuzen, and E. B. Goldstein (2020). chrisleaman/py-wave-runup: v0.1.10.

Lellouche, J.-M., E. Greiner, O. Le Galloudec, G. Garric, C. Regnier, M. Drevillon, M. Benkiran, C.-E. Testut, R. Bourdalle-Badie, F. Gasparin, et al. (2018). Recent updates to the Copernicus Marine Service global ocean monitoring and forecasting real-time 1/12 deg high-resolution system. *Ocean Science 14*(5), 1093–1126.

Nielsen, P. (2009). *Coastal and estuarine processes*, Volume 29. World Scientific Publishing Company.

Passarella, M., E. B. Goldstein, S. De Muro, and G. Coco (2018). The use of genetic programming to develop a predictor of swash excursion on sandy beaches. *Natural Hazards and Earth System Sciences 18*(2), 599–611.

Power, H. E., B. Gharabaghi, H. Bonakdari, B. Robertson, A. L. Atkinson, and T. E. Baldock (2019). Prediction of wave runup on beaches using gene-expression programming and empirical relationships. *Coastal Engineering 144*, 47–61.

Rovere, A. (2024). Beach ridges runup models for paleo sea level applications.

Ruggiero, P., P. D. Komar, W. G. McDougal, J. J. Marra, and R. A. Beach (2001). Wave runup, extreme water levels and the erosion of properties backing beaches. *Journal of coastal research*, 407–419.

Senechal, N., G. Coco, K. R. Bryan, and R. A. Holman (2011). Wave runup during extreme storm conditions. *Journal of Geophysical Research: Oceans 116*(C7).

Stockdon, H. F., R. A. Holman, P. A. Howd, and A. H. Sallenger (2006). Empirical parameterization of setup, swash, and runup. *Coastal Engineering 53*(7), 573–588.

Vos, K., M. D. Harley, K. D. Splinter, A. Walker, and I. L. Turner (2020). Beach Slopes From Satellite-Derived Shorelines. *Geophysical Research Letters 47*(14), e2020GL088365.

Vos, K., K. D. Splinter, M. D. Harley, J. A. Simmons, and I. L. Turner (2019). CoastSat: A Google Earth Engine-enabled Python toolkit to extract shorelines from publicly available satellite imagery. *Environmental Modelling & Software 122*, 104528.

Vousdoukas, M. I., D. Wziatek, and L. P. Almeida (2012). Coastal vulnerability assessment based on video wave run-up observations at a mesotidal, steep-sloped beach. *Ocean Dynamics 62*, 123–137.